

# Linear sea-level response to abrupt ocean warming of major West Antarctic ice basin

M. Mengel<sup>1,2</sup>, J. Feldmann<sup>1,2</sup> and A. Levermann<sup>1,2\*</sup>

**Antarctica's contribution to global sea-level rise has recently been increasing<sup>1</sup>. Whether its ice discharge will become unstable and decouple from anthropogenic forcing<sup>2-4</sup> or increase linearly with the warming of the surrounding ocean is of fundamental importance<sup>5</sup>. Under unabated greenhouse-gas emissions, ocean models indicate an abrupt intrusion of warm circumpolar deep water into the cavity below West Antarctica's Filchner-Ronne ice shelf within the next two centuries<sup>6,7</sup>. The ice basin's retrograde bed slope would allow for an unstable ice-sheet retreat<sup>8</sup>, but the buttressing of the large ice shelf and the narrow glacier troughs tend to inhibit such instability<sup>9-11</sup>. It is unclear whether future ice loss will be dominated by ice instability or anthropogenic forcing. Here we show in regional and continental-scale ice-sheet simulations, which are capable of resolving unstable grounding-line retreat, that the sea-level response of the Filchner-Ronne ice basin is not dominated by ice instability and follows the strength of the forcing quasi-linearly. We find that the ice loss reduces after each pulse of projected warm water intrusion. The long-term sea-level contribution is approximately proportional to the total shelf-ice melt. Although the local instabilities might dominate the ice loss for weak oceanic warming<sup>12</sup>, we find that the upper limit of ice discharge from the region is determined by the forcing and not by the marine ice-sheet instability.**

Sea-level rise poses a future challenge to coastal regions worldwide<sup>13</sup> and affects livelihoods and ecosystems in the most vulnerable regions already today<sup>14</sup>. Despite significant advances in ice-sheet modelling<sup>3,4,15-17</sup>, the largest uncertainty in future projections arises from the dynamics of the Antarctic ice sheet<sup>5</sup>. Ice shelves, the floating extensions of the ice sheet, modulate the ice-sheet flow through their back stress on the upstream glaciers, which is termed buttressing<sup>9</sup>. Although diminished shelves do not directly contribute to sea-level rise, the associated loss in buttressing can generate sea-level-relevant ice loss through the acceleration and thinning of upstream glaciers.

In addition to difficulties with the boundary conditions and the bed and ice rheology, the quantification of the future Antarctic ice flow is complicated through ice instability and potentially abrupt changes in ocean heat transport. First, marine-based ice sheets with retrograde bed slope can experience unstable grounding-line retreat<sup>8</sup>. It is, for example, hypothesized that the Amundsen sector has entered a state of unstable retreat triggered by increased melting beneath the ice shelves of Pine Island and Thwaites Glaciers<sup>3,4,18</sup>. Ice shelves play an important role in modulating the instability through their buttressing effect, with strong buttressing being able to inhibit unstable grounding-line retreat<sup>10,11</sup>.

Second, atmospheric changes may trigger the breakdown of the Antarctic slope front in the ocean off the Antarctic coast. At present,

most Antarctic ice shelves are surrounded by cold water masses near the freezing point. That is because the Antarctic slope front<sup>19</sup> acts as a barrier for heat and salt exchange with the northern warmer and saltier water masses. Projections of the breakdown of this front in ocean simulations under atmospheric warming<sup>6,7,20</sup> and under the southward shift of the Southern Westerlies<sup>21</sup> raise concerns that increased ocean heat transport towards the ice shelves will boost future ice loss from Antarctica. It is of fundamental importance for the projection of future sea-level rise to understand whether global warming can trigger abrupt ocean warming beneath the ice shelves and induce instability of marine-based ice sheets.

The tributary glaciers that feed the Filchner-Ronne ice shelf (FRIS, Fig. 1) rest on retrograde bed slope<sup>22</sup> that suggests that unstable ice retreat is possible<sup>8</sup>. High-resolution ice-sheet simulations show that some of the glaciers can undergo accelerating retreat when sub-shelf melting is sustained at increased levels<sup>12</sup>. However, the FRIS glaciers are highly buttressed by the large ice shelf, which can suppress unstable retreat<sup>9-11</sup>. A reduction in size and volume of the FRIS can be expected under the abrupt intrusion of warm water into the ice-shelf cavity that is indicated by ocean models<sup>6,7</sup>. It is unclear whether the strongly increased ice-shelf mass loss by the abrupt intrusion of warm water can induce the unstable retreat of the FRIS glaciers in a way that it will dominate the region's contribution to sea-level rise. The large buttressing ice shelf suggests a tight link between ice-shelf melting and sea-level-relevant ice-sheet mass loss. The FRIS glaciers may therefore respond differently to ice-shelf melting than the ice-sheet-instability-dominated Amundsen glaciers<sup>3,4</sup>.

We here investigate the response of the FRIS tributary glaciers to pulses of enhanced basal melting that are constructed from FESOM ocean projections<sup>7</sup> for the twenty-first and twenty-second century under the A1B scenario. The constructed pulses serve as boundary conditions for regional and continent-wide ice-sheet simulations with the Parallel Ice Sheet Model (PISM). Basal melting is pressure-adapted to the evolving ice-shelf thickness (see Supplementary Information). The pulses are applied to an ensemble of equilibrated ice-sheet states that show stable margins comparable to the observed ice fronts (Supplementary Figs 1 and 2). The ensemble represents perturbed ice-flow and basal-friction parameters under time-constant present-day atmosphere and repeatedly applied historic (1960–2000) ocean boundary conditions (Supplementary Tables 1 and 2). To our knowledge, this is the first time that cavity-resolving ocean simulations for the FRIS have been combined with dynamic ice-sheet simulations.

PISM (ref. 23; see Methods) applies the superposition of two shallow approximations of the stress balance to consistently simulate slow-moving grounded ice and the fast-flowing ice of outlet glaciers, ice streams and ice shelves, and is capable of modelling

<sup>1</sup>Potsdam Institute for Climate Impact Research, 14473 Potsdam, Germany. <sup>2</sup>Institute of Physics, Potsdam University, 14476 Potsdam, Germany.  
\*e-mail: anders.levermann@pik-potsdam.de

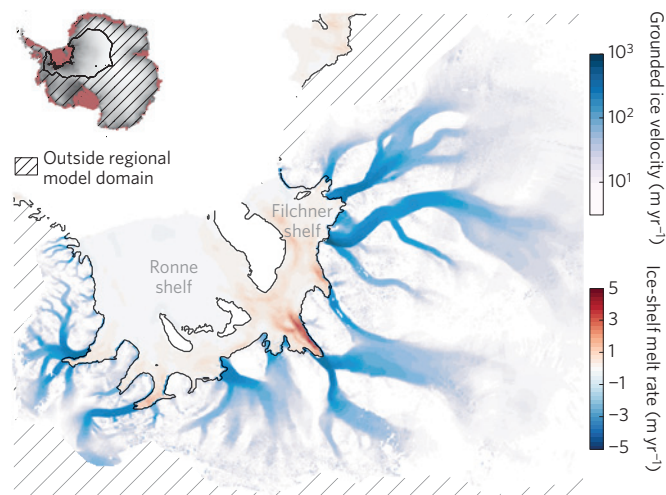


**Figure 1 | The Filchner-Ronne ice shelf and its tributary glaciers.** Ice velocity<sup>28</sup> (blue shading) for the grounded ice and basal melting from ocean simulations<sup>7</sup> (blue to red shading) for the floating ice shelf are shown. Grounded ice outside the regional model domain is hatched. Inset: the regional model domain on Antarctica, which is truncated in the East in the main panel. The observed grounding line<sup>22</sup> is indicated by the black line.

unstable grounding-line retreat<sup>24</sup>. A combination of thickness- and eigencaulving<sup>25</sup> allows dynamic calving fronts, which is especially important under strong ocean melting that can induce calving-front retreat.

The FESOM ocean model simulations<sup>7</sup> are driven by HadCM3 atmospheric data for the A1B scenario. The sub-shelf ocean temperature increases abruptly at the beginning of the twenty-first century, with a linear warming trend thereafter (Fig. 2a, blue line). The warming has a significant lag with respect to the global mean temperature increase (Fig. 2a, red line). A similar response to atmospheric warming with a different time lag has been identified with the predecessor of FESOM (ref. 6).

Average yearly FRIS mass loss in the ice-sheet simulations is around 90 Gt yr<sup>-1</sup> in equilibrium through the repeated historical melting and comparable to observations<sup>26</sup> (Supplementary Fig. 1). Linked to the warming, there are two periods of abrupt increase in melt loss at the beginning and the end of the twenty-second century towards more than 600 Gt yr<sup>-1</sup> and more than 2,000 Gt yr<sup>-1</sup> in the PISM scenario simulations (Fig. 2b, black line), representing an up to twentyfold increase. The increase is weaker than calculated in FESOM (ref. 7) because ice-shelf size already reduces in the course of the twenty-second century. The sea-level-relevant ice loss is negligible in the twenty-first century and accelerates towards the end of the twenty-second century, where it reaches around 6 cm (Fig. 2b, green line). As the ocean forcing ends in 2200, a further acceleration of basal melting and ice loss after 2200 cannot be ruled out.

Because of the significant uncertainty associated with the timing and length of the warm water intrusion, sensitivity experiments with melt rates from the decades 2040–2050, 2100–2110, 2140–2150 and 2190–2200 (Fig. 2, grey bars) are conducted to represent levels of potential future abrupt ocean warming. These melting conditions are then applied for different time lengths of 40, 80, 160 and 320 years below the FRIS with equilibrium conditions applied afterwards.

The presented results are based on a combination of regional (5-km resolution) and continental-scale (12-km resolution) simulations. Whereas the regional simulations better represent the ice flow, especially close to the grounding line, the continental simulations have no boundary effects and guarantee that the chosen parameter combinations are consistent with observed Antarctic conditions (Supplementary Figs 1 and 2). Both set-ups yield the same qualitative and quantitative results.

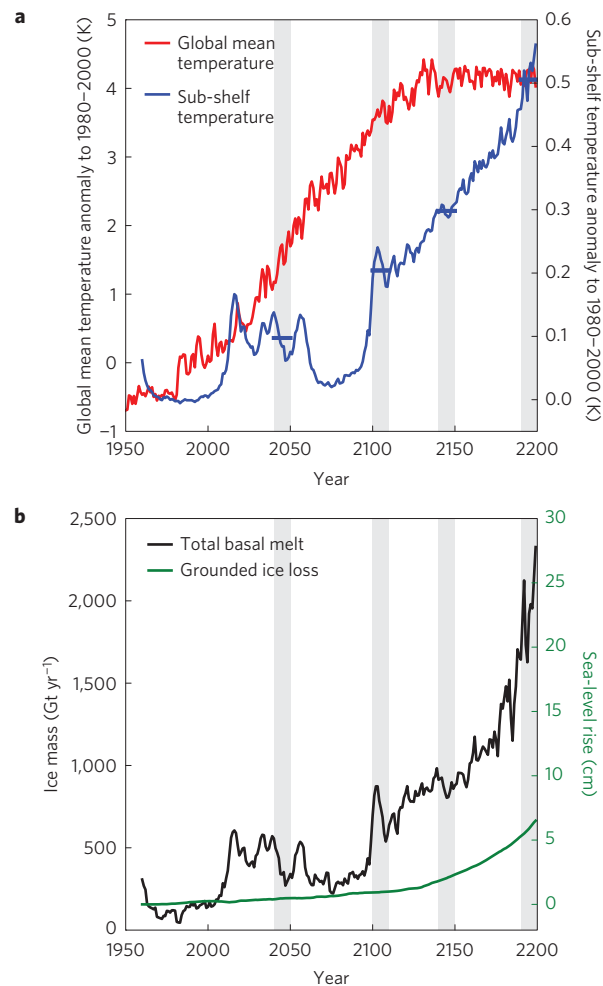


**Figure 2 | Global mean and Antarctic subsurface ocean warming.** **a**, Time series of global mean temperature as projected under the A1B scenario with the HadCM3 AOGCM (red line) and mean ocean subsurface temperature under FRIS from HadCM3-driven FESOM (blue line). **b**, Simulated total ice loss rate through basal melt and sea-level-relevant ice loss under the A1B scenario.

We find that the retreat of the ice sheet is predominantly driven by the external forcing and not by an internal self-sustaining instability. This can be inferred from two observations. First, the sea-level-relevant mass loss slows down after the end of the forcing for all levels of melting (Fig. 3, compare different coloured lines) and all forcing lengths (Fig. 3, compare the panels). For end of twenty-second century forcing (red lines), regional simulations (thick lines) show less ice mass loss for the 160-yr and 320-yr pulses than whole-continent simulations (thin lines), because the spreading of the thinning interferes with the model boundaries. Most simulations equilibrate within the simulation time of 1,000 yr, although some forced by strong end-of-twenty-second-century melting show continued ice loss.

Second, the overall sea-level-relevant mass loss after 1,000 yr (Fig. 4, *y*-axis) increases quasi-linearly with the cumulative anomalous ice-shelf melting (Fig. 4, *x*-axis) for strong melting, although a weaker response (dashed black line) is found for weak forcing. The slope of the linear fit for all experiments (full black line) is 1.7 mm sea-level rise per 1,000 Gt of anomalous ice-shelf melting. For comparison, 1,000 Gt of grounded ice would raise sea level by 2.7 mm. None of the weakly forced experiments exhibits sea-level-relevant ice loss of a magnitude similar to the strongly forced experiments. Hence, although ice instabilities may be present

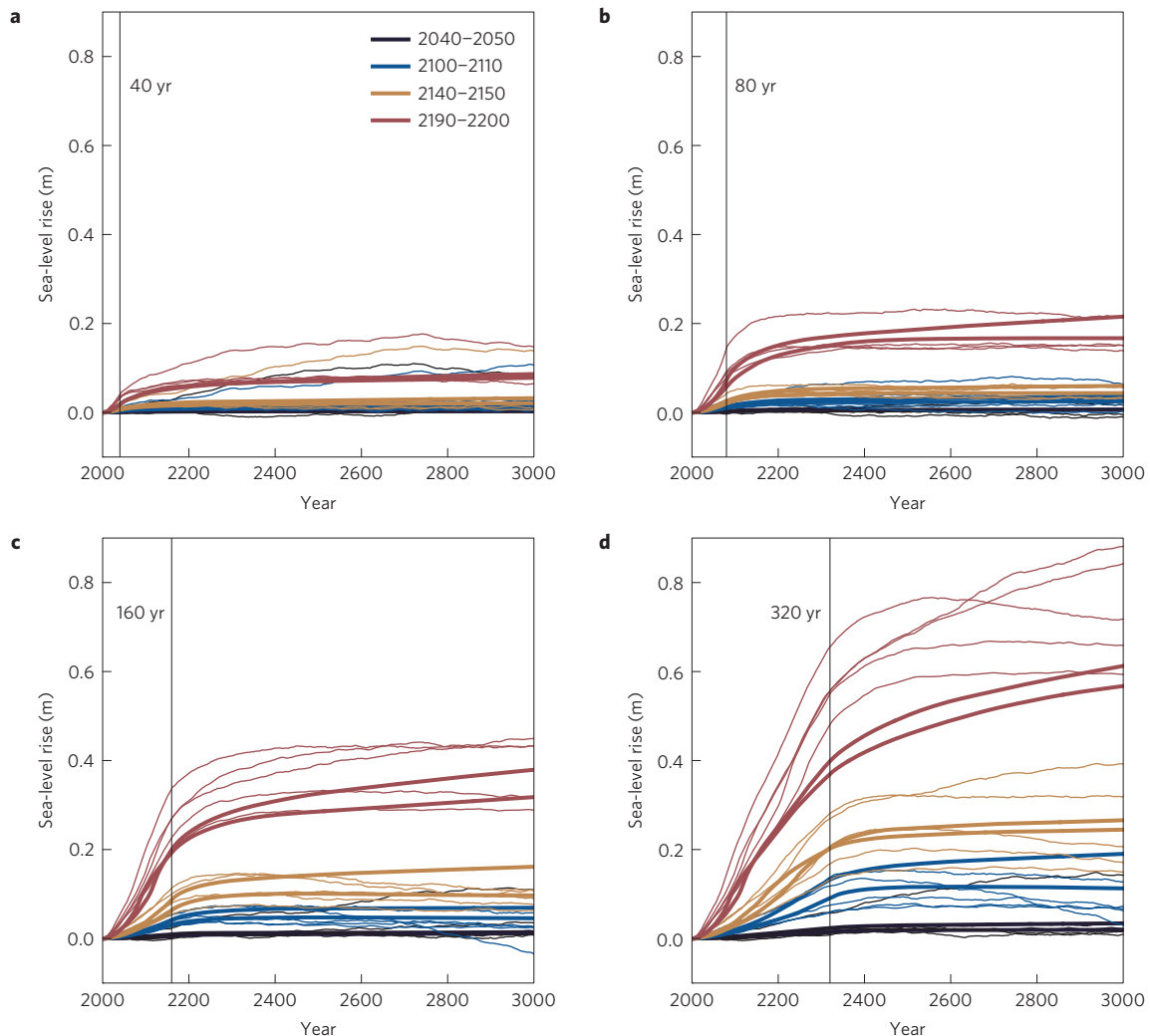


**Figure 3 | Response to ocean melt pulses.** Ice-sheet response to pulses of ocean melt rates as projected by FESOM for different time periods (indicated by the coloured lines). Pulse lengths 40 yr (**a**), 80 yr (**b**), 160 yr (**c**) and 320 yr (**d**). Thin lines indicate whole-continent simulations and thick lines indicate regional simulations.

in the FRIS tributary glaciers, the forcing-induced losses dominate the discharge.

Ice plains are regions of grounded ice close to flotation. The ungrounding of the ice plains as part of the Institute and Möller ice streams determine the sensitivity to the melt forcing. For weak forcing below 100,000 Gt integrated anomalous melt, the ice plains stay grounded for all regional simulations, leading to a lower sensitivity of approximately 1.1 mm sea-level rise per 1,000 Gt of anomalous melt (Fig. 4 dashed black line). If the ungrounding occurs, which is true for all regional ensemble members with forcing beyond 110,000 Gt, the sensitivity to melt forcing increases, leading to the linear relation of 1.7 mm per 1,000 Gt of anomalous melting (full black line). We illustrate the difference between a forced state with stable ice plains and ungrounded ice plains (indicated by the black and red cross respectively in Fig. 4) in Supplementary Fig. 3.

Our findings are based on unidirectionally coupled ocean-to-ice-sheet simulations, thus introducing a number of caveats. The changes of ice-shelf geometry do not feed back to the ocean model and it cannot be ruled out that such changes have an effect on the ocean circulation. Ice-shelf slope influences the melting and we do not account for such a dependence<sup>27</sup>. Slope dependence potentially strengthens the applied melting and therefore does not contradict our findings. Because the ocean model has been run with a static ice-shelf model, the influence of ice-shelf melt water is accounted

for in the ocean simulations, but the local anomalies introduced by changes in ice-shelf extent and thickness are not. When the grounding line retreats, the melting may occur at deeper waters than in the ocean model configuration, and the higher pressure leads to increased melting. However, for the late twenty-second century, when the retreat occurs, the area-integrated basal melting, as derived in the ice-sheet model (Fig. 2, black line), is lower than the FESOM values (ref. 7, their Fig. 7, upper left panel, pink line). This is due to the overall reduced ice-shelf size and thickness in response to the forcing, and shows that we do not overestimate the large-scale oceanic heat transport to the ice shelf. As oceanic conditions in regions covered at present by land ice are unknown, we filled missing ocean data by simple diffusion into regions below sea level, leading to water properties further inland that are similar to the FRIS-cavity water properties. The assumption that the water mass can reach the previously land-ice-covered regions undiluted may overestimate the melting locally.

Despite these caveats, it can be concluded that the maximum ice discharge that can be expected from the FRIS region is not dominated by the marine ice-sheet instability, but by the oceanic heat transport towards the ice shelf. Although many physical systems exhibit quasi-linear behaviour for weak perturbations, and show nonlinearities mainly for increased forcing, this is not the case for the FRIS region. In situations where the timescale that is

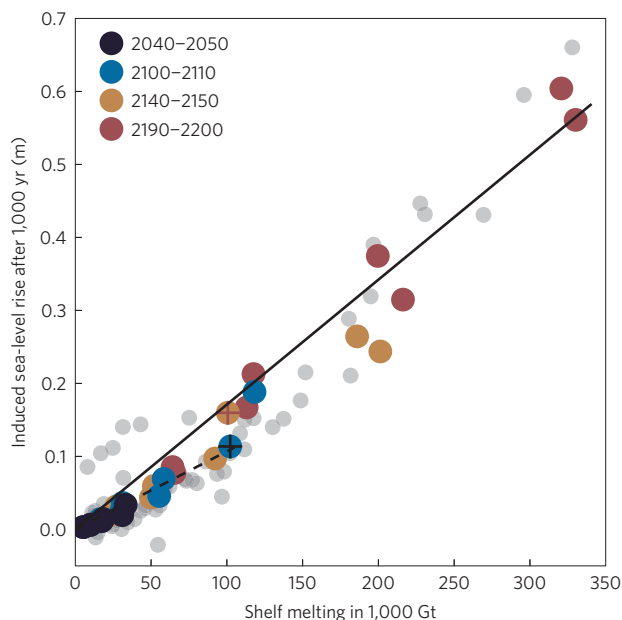


**Figure 4 | Linear response to total melt.** Induced sea-level rise for the integrated amount of anomalous melting as predicted in the ice-sheet model. Coloured dots show regional simulations, with colours indicating different melting periods. Grey dots are whole-continent simulations. The linear fit for all experiments is shown as a full black line. The dashed line indicates the fit for the weaker response under weak forcing. The difference between the linearly responding (red cross) and less sensitive state (black cross) is illustrated in Supplementary Fig. 3.

associated with an instability is much larger than the timescale of the applied forcing, a quasi-linear behaviour is found for strong perturbations whereas weak forcing may uncover a nonlinear response. It can be speculated that such situations exist more often in cryospheric systems under fast anthropogenic warming.

## Methods

Methods and any associated references are available in the [online version of the paper](#).

Received 10 December 2014; accepted 18 August 2015; published online 5 October 2015

## References

1. Shepherd, A. *et al.* A reconciled estimate of ice-sheet mass balance. *Science* **338**, 1183–1189 (2012).
2. Schoof, C. Ice sheet grounding line dynamics: Steady states, stability, and hysteresis. *J. Geophys. Res.* **112**, F03S28 (2007).
3. Favier, L. *et al.* Retreat of Pine Island Glacier controlled by marine ice-sheet instability. *Nature Clim. Change* **4**, 117–121 (2014).
4. Joughin, I., Smith, B. E. & Medley, B. Marine ice sheet collapse potentially under way for the Thwaites Glacier Basin, West Antarctica. *Science* **344**, 735–738 (2014).
5. IPCC *Climate Change 2013: The Physical Science Basis* (eds Stocker, T. F. *et al.*) (Cambridge Univ. Press, 2014); <http://www.climatechange2013.org/report/full-report>
6. Hellmer, H. H., Kauker, F., Timmermann, R., Determann, J. & Rae, J. Twenty-first-century warming of a large Antarctic ice-shelf cavity by a redirected coastal current. *Nature* **485**, 225–228 (2012).
7. Timmermann, R. & Hellmer, H. H. Southern Ocean warming and increased ice shelf basal melting in the twenty-first and twenty-second centuries based on coupled ice-ocean finite-element modelling. *Ocean Dynam.* **63**, 1011–1026 (2013).
8. Ross, N. *et al.* Steep reverse bed slope at the grounding line of the Weddell Sea sector in West Antarctica. *Nature Geosci.* **5**, 393–396 (2012).

9. Dupont, T. K. & Alley, R. B. Assessment of the importance of ice-shelf buttressing to ice-sheet flow. *Geophys. Res. Lett.* **32**, L04503 (2005).
10. Gudmundsson, G. H., Krug, J., Durand, G., Favier, L. & Gagliardini, O. The stability of grounding lines on retrograde slopes. *Cryosphere* **6**, 1497–1505 (2012).
11. Gudmundsson, G. H. Ice-shelf buttressing and the stability of marine ice sheets. *Cryosphere* **7**, 647–655 (2013).
12. Wright, A. P. *et al.* Sensitivity of the Weddell Sea sector ice streams to sub-shelf melting and surface accumulation. *Cryosphere* **8**, 2119–2134 (2014).
13. Hirabayashi, Y. *et al.* Global flood risk under climate change. *Nature Clim. Change* **3**, 816–821 (2013).
14. IPCC *Climate Change 2014: Impacts, Adaptation, and Vulnerability* (eds Field, C. B. *et al.*) (Cambridge Univ. Press, 2014); <https://ipcc-wg2.gov/AR5/report/full-report>
15. Goelzer, H. *et al.* Millennial total sea-level commitments projected with the Earth system model of intermediate complexity LOVECLIM. *Environ. Res. Lett.* **7**, 045401 (2012).
16. Gladstone, R. M. *et al.* Calibrated prediction of Pine Island Glacier retreat during the 21st and 22nd centuries with a coupled flowline model. *Earth Planet. Sci. Lett.* **333–334**, 191–199 (2012).
17. Seroussi, H. *et al.* Sensitivity of the dynamics of Pine Island Glacier, West Antarctica, to climate forcing for the next 50 years. *Cryosphere* **8**, 1699–1710 (2014).
18. Rignot, E., Mouginot, J., Morlighem, M., Seroussi, H. & Scheuchl, B. Widespread, rapid grounding line retreat of Pine Island, Thwaites, Smith, and Kohler glaciers, West Antarctica, from 1992 to 2011. *Geophys. Res. Lett.* **41**, 3502–3509 (2014).
19. Jacobs, S. S. On the nature and significance of the Antarctic Slope Front. *Mar. Chem.* **35**, 9–24 (1991).
20. Petty, A. A., Feltham, D. L. & Holland, P. R. Impact of atmospheric forcing on Antarctic continental shelf water masses. *J. Phys. Oceanogr.* **43**, 920–940 (2013).
21. Spence, P. *et al.* Rapid subsurface warming and circulation changes of Antarctic coastal waters by poleward shifting winds. *Geophys. Res. Lett.* **41**, 4601–4610 (2014).
22. Fretwell, P. *et al.* Bedmap2: Improved ice bed, surface and thickness datasets for Antarctica. *Cryosphere* **7**, 375–393 (2013).
23. Bueler, E. & Brown, J. Shallow shelf approximation as a ‘sliding law’ in a thermomechanically coupled ice sheet model. *J. Geophys. Res.* **114**, F03008 (2009).
24. Mengel, M. & Levermann, A. Ice plug prevents irreversible discharge from East Antarctica. *Nature Clim. Change* **4**, 451–455 (2014).
25. Levermann, A. *et al.* Kinematic first-order calving law implies potential for abrupt ice-shelf retreat. *Cryosphere* **6**, 273–286 (2012).
26. Moholdt, G., Padman, L. & Fricker, H. A. Basal mass budget of Ross and Filchner-Ronne ice shelves, Antarctica, derived from Lagrangian analysis of ICESat altimetry. *J. Geophys. Res.* **119**, 2361–2380 (2014).
27. Little, C. M., Gnanadesikan, A. & Oppenheimer, M. How ice shelf morphology controls basal melting. *J. Geophys. Res.* **114**, C12007 (2009).
28. Rignot, E., Mouginot, J. & Scheuchl, B. Ice flow of the Antarctic ice sheet. *Science* **333**, 1427–1430 (2011).

## Acknowledgements

The study was partially financially supported by the Deutsche Forschungsgemeinschaft (DFG) and the German Federal Environmental Foundation (DBU). We are grateful to R. Timmermann for providing the FESOM ocean model data. Model development for PISM at the University of Alaska, Fairbanks, USA was supported by the NASA grants NNX13AM16G and NNX13AK27G.

## Author contributions

M.M., J.F. and A.L. designed the study and wrote the text. M.M. and J.F. conducted the model simulations. M.M. prepared the figures.

## Additional information

Supplementary information is available in the [online version of the paper](#). Reprints and permissions information is available online at [www.nature.com/reprints](http://www.nature.com/reprints). Correspondence and requests for materials should be addressed to A.L.

## Competing financial interests

The authors declare no competing financial interests.

## Methods

We here use the continental-scale Parallel Ice Sheet Model (PISM; refs 23,29,30) to explore the response of the Antarctic ice sheet to ocean conditions as projected within the next 200 years in the high-resolution Finite Element Southern Ocean Model (FESOM; ref. 7). The ocean model is driven by atmospheric conditions from the HadCM3 global climate model under A1B scenario forcing. To isolate the response of the Filchner–Ronne Ice Shelf (FRIS) we combine the A1B scenario data for the Weddel Sea with twentieth-century data for the rest of the Antarctic coastal waters.

The transition zone between sheet and shelf is not parametrized in PISM and can fully adapt to changes in ice flow and geometry<sup>30</sup>. The local interpolation of grounding-line position and basal friction, coupled with a specific driving stress scheme at the grounding line, make PISM capable of modelling reversible grounding-line motion in the MISIP3d experiments<sup>31</sup> comparable to the results obtained from full Stokes flow<sup>32</sup>.

We use a combination of regional and whole-continent simulations to retain high accuracy for grounding-line movement while controlling for the effects of regional domain boundaries. Regional simulations of the FRIS catchment basin are carried out on 5-km resolution. A set of stable equilibrium states for the whole Antarctic ice sheet was created on 12-km resolution. All simulations show stable ice-sheet margins in equilibrium, comparable to present day (Supplementary Figs 1 and 2). Uncertainties are covered by the variation of basal-friction and

ice-flow parameters and calving parameters (see Supplementary Text and Supplementary Tables 1 and 2).

We apply a simple pressure-adaption of the ocean melting rates in PISM to account for local shelf thickness change (see Supplementary Information). Ocean melting is also applied to an area fraction of the grid boxes containing ice grounded below sea level and adjacent to the ocean through a buoyancy-dependent basal-melt interpolation scheme.

## References

- Winkelmann, R. *et al.* The Potsdam Parallel Ice Sheet Model (PISM-PIK)—Part 1: Model description. *Cryosphere* **5**, 715–726 (2011).
- Martin, M. A. *et al.* The Potsdam Parallel Ice Sheet Model (PISM-PIK)—Part 2: Dynamic equilibrium simulation of the Antarctic ice sheet. *Cryosphere* **5**, 727–740 (2011).
- Pattyn, F. *et al.* Grounding-line migration in plan-view marine ice-sheet models: Results of the ice2sea MISIP3d intercomparison. *J. Glaciol.* **59**, 410–422 (2013).
- Feldmann, J., Albrecht, T., Khroulev, C., Pattyn, F. & Levermann, A. Resolution-dependent performance of grounding line motion in a shallow model compared with a full-Stokes model according to the MISIP3d intercomparison. *J. Glaciol.* **60**, 353–360 (2014).